SPACE WEATHER, VOL. 4, S09005, doi:10.1029/2005SW000207, 2006

Predicting Solar Cycle 24 and beyond

Mark A. Clilverd,[1] Ellen Clarke,[2] Thomas Ulich,[3] Henry Rishbeth,[4] and Martin J. Jarvis[1]

Received 9 November 2005; revised 27 April 2006; accepted 28 April 2006; published 28 September 2006.

[1] We use a model for sunspot number using low-frequency solar oscillations, with periods 22, 53, 88, 106, 213, and 420 years modulating the 11-year Schwabe cycle, to predict the peak sunspot number of cycle 24 and for future cycles, including the period around 2100 A.D. We extend the earlier work of Damon and Jirikowic (1992) by adding a further long-period component of 420 years. Typically, the standard deviation between the model and the peak sunspot number in each solar cycle from 1750 to 1970 is ±34. The peak sunspot prediction for cycles 21, 22, and 23 agree with the observed sunspot activity levels within the error estimate. Our peak sunspot prediction for cycle 24 is significantly smaller than cycle 23, with peak sunspot numbers predicted to be 42 ± 34. These predictions suggest that a period of quiet solar activity is expected, lasting until ~2030, with less disruption to satellite orbits, satellite lifetimes, and power distribution grids and lower risk of spacecraft failures and radiation dose to astronauts. Our model also predicts a recovery during the middle of the century to more typical solar activity cycles with peak sunspot numbers around 120. Eventually, the superposition of the minimum phase of the 105- and 420-year cycles just after 2100 leads to another period of significantly quieter solar conditions. This lends some support to the prediction of low solar activity in 2100 made by Clilverd et al. (2003).

Citation: Clilverd, M. A., E. Clarke, T. Ulich, H. Rishbeth, and M. J. Jarvis (2006), Predicting Solar Cycle 24 and beyond, *Space Weather*, *4*, S09005, doi:10.1029/2005SW000207.

1. Introduction

[2] Solar activity, often defined by sunspot number, disturbs near-Earth plasmas, and as a result affects man-made systems in many varied ways (see *Gorney* [1990] for a review). Periodicities in solar activity can influence the frequency and intensity of space weather events, although individual severe space weather events can occur at any level of solar activity given by sunspot number, for example, fast solar wind streams which can cause satellite anomalies. However, increased solar activity through EUV irradiance reduces the lifetime of low-Earth-orbiting satellites by increasing the neutral density of the atmosphere (~150–1000 km) [*Walterscheid*, 1989]. Geomagnetic storms closely follow solar activity changes and also produce short-term variations in neutral density, perturbing orbital motions and reentry conditions. Further, ionospheric current systems are enhanced during geomagnetic storms and can induce electrical currents in large-scale man-made conductors such as oil pipelines and power distribution grids, producing such effects as the Hydro-Quebec blackout in March 1989 [*Boteler*, 2003]. Energetic particle effects on spacecraft and astronauts also respond to solar activity changes, both through direct emission of particles from the Sun and the acceleration of particles in the magnetosphere. Increased solar activity is associated with the increased probability of spacecraft failures as a result of charging events, degradation of solar cell performance, and increased radiation dose to space travelers [*Shea and Smart*, 1998].

[3] The clearest periodicity exhibited by solar activity is the quasi-11-year Schwabe cycle. However, over longer timescales, many other periods influence the overall levels of solar activity [*Damon and Jirikowic*, 1992; *Beer*, 2000]. Over much of the last 100 years, solar activity has shown an increasing trend following a quiet period at the beginning of the 1900s [*Lockwood et al.*, 1999; *Clilverd et al.*, 2003]. Will these high levels of solar activity continue, or should we expect a period of low solar activity in the future?

[4] The challenge of predicting solar activity has been considered by many authors [*Kane*, 2001, and references therein]. More than 20 estimates of the maximum level of

[1]British Antarctic Survey, Natural Environment Research Council, Cambridge, UK.
[2]British Geological Survey, Natural Environment Research Council, Edinburgh, UK.
[3]Sodankylä Geophysical Observatory, University of Oulu, Sodankylä, Finland.
[4]School of Physics and Astronomy, University of Southampton, Southampton, UK.

monthly smoothed sunspot number were made for Solar Cycle 23. Generally, the sunspot cycle was predicted to be of moderate size, with peak sunspot numbers ranging from 80 to 210. As it is now known, cycle 23 reached a maximum of 122, and several predictions were notably close (*Schatten et al.* [1996], *Ahluwalia* [1998], and *Conway et al.* [1998], to name a few). These techniques use a range of solar dynamo, neural networks, and quasiperiodicity studies.

[5] Several predictions have been made for cycle 24. *Echer et al.* [2004] used an extrapolation of sunspot number spectral components to predict cycle 24 as about 115. *De Meyer* [2003] used a semiempirical transfer function model of solar cycles to predict cycle 24 as 95–125. *Schatten* [2003] used a solar dynamo amplitude method to predict a peak sunspot number of about 100 for cycle 24. *Dikpati et al.* [2006] used a solar flux transport dynamo-based model to correctly "forecast" the peaks of previous cycles (16–23), predicting cycle 24 to be about 170 ± 12, a value primarily based on polar fields older than the previous cycle's. *Gholipour et al.* [2005] estimated a peak sunspot number of about 145 using neurofuzzy modeling. In contrast, *Badalyan et al.* [2001] used cyclic variations of the coronal green line intensities to predict peak sunspot levels of 50, while *Svalgaard et al.* [2005] used the strength of large-scale solar dynamo polar fields in cycle 23 to predict cycle 24 as 75 ± 8 at the peak. These latter two predictions would represent a very quiet solar cycle.

[6] Long-term trends in solar activity have also been considered by other workers using proxy datasets such as C^{14} [*Stuiver et al.*, 1998]. Following a superposed epoch analysis of C^{14} data, *Clilverd et al.* [2003] suggested that cycle 24 would be similar to previous cycles in amplitude, with low activity levels not being reached until 2100 A.D. This was mainly because of a 420-year repetition of the low-activity conditions following the Maunder Minimum of 1700. In contrast, *Usoskin et al.* [2003] used Be^{10} analysis to suggest that we are currently in a prolonged period of exceptionally high solar activity with little suggestion of lower activity levels to come.

[7] On the basis of earlier work by *Sonett* [1982], solar activity was modeled by *Damon and Jirikowic* [1992] as a low-frequency harmonic oscillator. In their analysis of C^{14} they developed a model of the modulation of the 11-year Schwabe carrier by longer periods (52.9, 88.1, 105.8, and 212.5 years). The model results fitted the sunspot activity series from 1700 to 1970 well, although the authors noted that the activity minimum at the beginning of the 1900s was modeled poorly, possibly because of the need for even longer periods to be included.

[8] More recently, *Vasillev and Dergachev* [2002] carried out a bispectrum analysis of the solar activity modulated C^{14} series and found that periods of 210, 420, and 710 years are the fundamental century-scale features in the data. In this study we extend the low-frequency modulation model developed by *Damon and Jirikowic* [1992] to include an additional period of 420 years optimized against the sunspot data from 1750–1970. The 420-year period is understood to be related to changes in the solar convective zone [*Stuiver and Braziunas*, 1989]. The results from the model for cycles 21–23 are used as a test. We then use the model to predict the amplitude of cycle 24 as well as to compare with the predictions for 2100 A.D. made by *Clilverd et al.* [2003].

2. Low-Frequency Modulation Model

[9] *Damon and Jirikowic* [1992] found a reasonable fit to the observed annual Wolf sunspot number using a squared low-frequency modulation model using the periods, 52.9, 88.1, 105.8, and 212.5 years. These represent the periods and overtones of the Suess (212-year) and Gleissberg (88-year) periods. Their analysis was based on the power spectrum of the radiocarbon ΔC^{14} series, which is modulated by solar activity. The Suess and Gleissberg periods are well-known solar cycles believed to be generated from the solar dynamo [*De Jager*, 2005, and references therein]. *Sonett* [1982] showed that by including a Gleissberg period [*Gleissberg*, 1966] in the amplitude modulation model all the spectral lines with period <88 years in the sunspot number series are reproduced, including the quasi-three-cycle periodicity used so successfully by *Ahluwalia* [1998] to predict the size of cycle 23. The most significant amplitude is for the 105.8-year cycle, which is approximately twice the amplitude of the 52.9- and 88.1-year cycles. Interestingly, the form of the model suggests that if the long-term periods were not present, then the sunspot number would remain at zero, in other words, in the Maunder Minimum state instead of with a predominant 11-year cycle.

[10] The form of the low-frequency modulation model was defined by *Damon and Jirikowic* [1992] as

$$R_z = \alpha_c \cos^2(\omega_c t + \phi_c) \sum_{i=1}^{6} \alpha_i \cos^2(\omega_i t + \phi_i) \quad (1)$$

alternatively written as

$$R_z = {}^1\!/_4 \alpha_c [1 + \cos 2(\omega_c t + \phi_c)] \sum_{i=1}^{6} \alpha_i [1 + \cos 2(\omega_i t + \phi_i)] \quad (2)$$

where the Zürich sunspot number is R_z, amplitude is α, frequency is ω, and phase is ϕ. This function has the form of the Schwabe 11.1-year carrier signal c, modulated by the low-frequency cycles $i = 1-6$,

$$R_z = A(t) \cos^2(2\omega_c t + \phi_c) \quad (3)$$

[11] The amplitude of the carrier signal c is not just α_c (as one might expect at first), but a slowly varying function $A(t)$ with mean value $1.5\alpha_c$, containing the cycles 1–6. Note that in these equations, all the angular frequencies correspond to twice the period of the oscillations. Thus, for

Table 1. Cycle Parameters for the Low-Frequency Modulation Model[a]

Cycle	Period, years	Amplitude	Phase, years
Carrier	11.1	65.4	1.46
1 (new cycle)	22.2	0.2	1.0
2	52.9	0.66	0.62
3	88.1	0.43	−1.82
4	105.8	1.31	1.10
5	212.5	0.01	1.33
6 (new cycle)	420.0	0.45	−1.0

[a]Cycles 2−5 are from *Damon and Jirikowic* [1992].

the Schwabe carrier period of 11.1 years, $\omega_c = 2\pi/22.2\ \mathrm{yr}^{-1}$ and similarly for ω_{1-6}, while the parameters α_c and α_{1-5} represent twice the amplitudes of the oscillations. The parameters are shown in Table 1, those for $i = 2-5$ and c being as defined by *Damon and Jirikowic* [1992].

[12] Using the model, it is possible to add an additional 22-year period. By averaging the peak sunspot number from the odd and even cycles (0−23), it was apparent that the odd cycles were larger by ~13. Thus the 22-year period would have a small amplitude, influencing the model results at a level less than the standard deviation. However, if all the other amplitudes in Table 1 were to fall to zero, then the model would represent a Grand Minimum with a small-residue 22-year cycle if that were included.

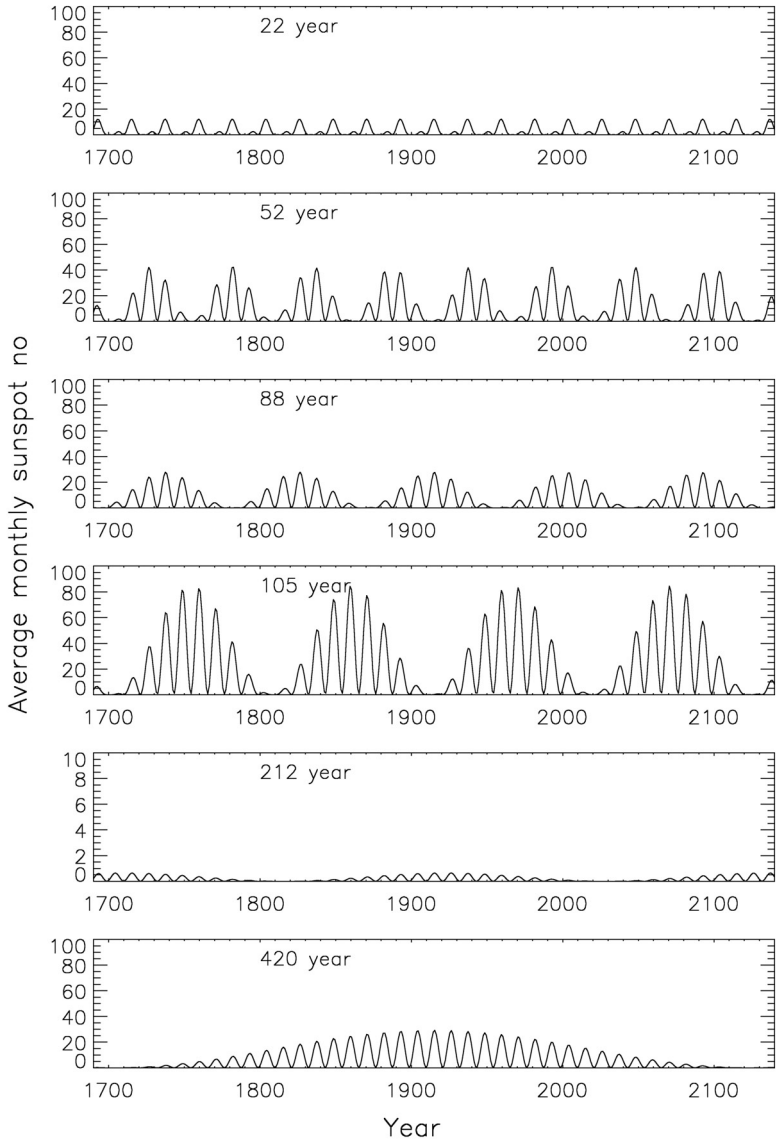

Figure 1. Individual effect of each modulation period on the 11.1-year Schwabe cycle during the period 1690−2140.

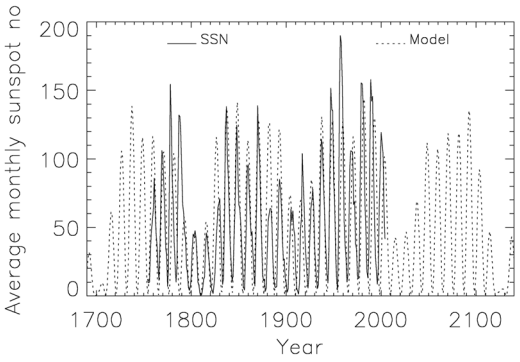

Figure 2. Variation of the average monthly sunspot number since 1750 compared with the results from the low-frequency modulation model of equation (1).

This picture would be consistent with conditions in the Maunder Minimum [*Kovaltsov et al.*, 2004].

[13] We have also added the 420-year cycle ($i = 6$) to the model by determining amplitude through fitting the model to the sunspot number series from 1750 to 1970, as in the work by *Damon and Jirikowic* [1992]. The amplitude of the 420-year cycle is close to that of the 52.9- and 88.1-year cycles. The phase of the 420-year cycle is such that the smallest modulation product of the Schwabe carrier was in 1700—the Maunder Minimum—and the largest modulation product was just after 1900; that is, the 420-year cycle is phase locked to the Maunder Minimum. In Figure 1 we show, for the period 1690–2140, the relative amplitudes of the cycles shown in Table 1. Note that the 212-year cycle amplitude range is one tenth of that in the other plots.

[14] Figure 2 shows the comparison between sunspot number (solid line) and the low-frequency modulation model (dashed line). A few features are apparent. The periods of low solar activity in about 1805 and 1910 are better represented with the inclusion of the 420-year cycle. The trend in modeled sunspot number during the 1900s is generally one of an increase in activity agreeing with observations and many previous reports [*Lockwood et al.*, 1999; *Cliver et al.*, 1998; *Clilverd et al.*, 1998]. However, individual cycles with very high activity levels, e.g., cycle 19 (1955–1964), are not particularly well represented. It is interesting to note here that the model indicates a peak sunspot number of 102 ± 34 for cycle 23, which encompasses the actual value.

[15] Figure 2 shows the low-frequency modulation model results for the whole of the period 1700–2130. The small solar cycles in 1805 and 1910 are well represented in the model, and because of the strength of the 105.8-year oscillation in particular, the next solar cycle (24) is also expected to be small. The peak sunspot number should only reach 40–50, which is equivalent to the activity levels associated with the Dalton Minimum of 1805. Cycle 25 is also predicted to be small, but the subsequent cycles recover to levels more typical of cycles 17, 20, and 23, i.e., peak sunspot numbers of about 120. Ultimately, the model shows a significant decrease in activity after 2100 because of the strong 105.8-year cycle and the phasing of

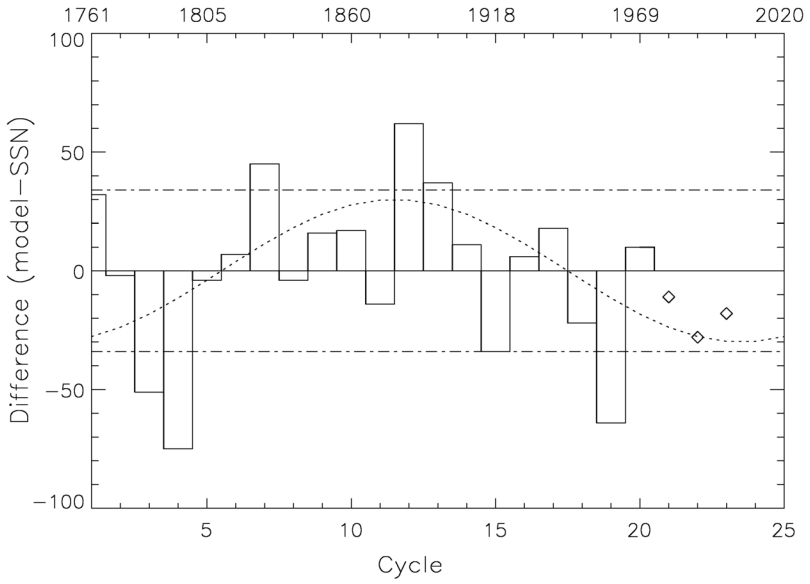

Figure 3. Difference in observed peak sunspot number compared with the model prediction for each 11.1-year solar cycle for the comparison period 1750–1970. The three diamonds represent the difference between the model and observations for cycles after 1970 (21, 22, and 23). The dash-dotted lines indicate a likely sinusoidal trend in the mismatch between model and observations.

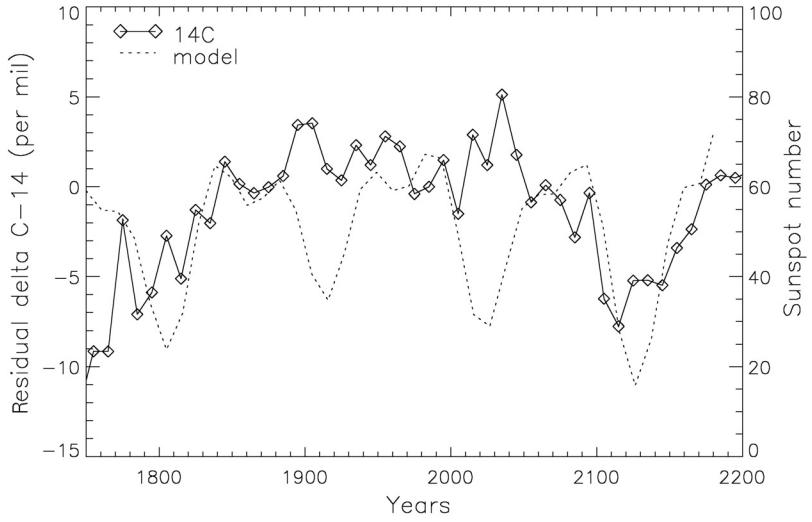

Figure 4. Comparison between the solar cycle averaged sunspot number from the low-frequency modulation model (dashed line) and the superposed C^{14} variation (diamonds) after a Maunder-like minimum from *Clilverd et al.* [2003].

the 420-year cycle. As a result, the expected peak sunspot number is very low.

[16] The difference between the peak sunspot number for each cycle during the period 1750–1970 and the output of the amplitude oscillation model is shown in Figure 3. Three diamonds represent the difference between the model and observations for the test cycles after 1970 (21, 22, and 23). Typically, the model underestimated the peak activity of cycles 21–23 by ~20, which is within the standard deviation estimate of ±34. Dash-dotted lines are included on the plot to indicate a possible sinusoidal variation in the offset between model and observations. The line suggests that, as in recent cycles, the model is likely to underestimate the peak sunspot numbers by 20–30 in future cycles. As noted above, there have also been several cycles where the difference in predicted and observed sunspot number is large (>50), which appear to occur every seven cycles or so, with the last occurring in cycle 19. Clearly, the model does not include this behavior, as it is not cyclic. From cycles 1–20, the average standard deviation of the model from the sunspot number has been ±34, with a close balance of overestimates and underestimates. Because this technique uses an unchanging 11.1-year period for the Schwabe cycle, no inference can be made about the timing of the peak.

[17] The results from the low-frequency oscillation model can also be compared with the results from the long-term predictions made by *Clilverd et al.* [2003]. Figure 4 replots the data from Figure 3 of *Clilverd et al.* [2003], in which the superposed C^{14} residual variation was scaled against average sunspot number. Here that line is represented by joined diamonds. These data were the basis for the prediction of low solar activity in 2100. The dashed line in Figure 4 shows the solar cycle averaged sunspot number from the model. It is clear that the model and the C^{14} analysis show similarities over the whole period plotted and in predicting a minimum in solar activity just after 2100. The main feature that the model includes is the strong ~100-year period, which is missing in the C^{14} analysis. It should be noted that the C^{14} data for the period 1700–1900 responds to the 1805 Dalton Minimum reasonably well, but this feature does not stand out when superposing the recovery periods from previous Maunder Minimum conditions. Thus we can understand why *Clilverd et al.* [2003] predicted similar solar activity levels in cycle 24 to cycle 23 rather than a significantly smaller cycle as we predict now. We can also see that from about 2050 the two techniques return to a degree of agreement.

3. $F_{10.7\ cm}$ Flux and Solar Activity Effects

[18] It is relatively simple to convert the sunspot model results into solar radio flux ($F_{10.7\ cm}$) as they correlate well. The radio flux can be measured relatively easily and is used as an index of solar activity for many purposes. Figure 5 shows the sunspot model results converted to annual average $F_{10.7}$ flux, compared with the observed values from 1947–2004. The agreement is generally good apart from the peaks of cycles 19 and 20 where there are differences of ±50 (plus for cycle 19, minus for 20). The predicted $F_{10.7\ cm}$ flux levels for the peak of cycle 24 is only around 100 instead of the more typical 200.

[19] Lower solar activity in cycle 24 will produce a range of effects in the Earth's atmosphere. It should reduce the solar UV forcing of the upper stratosphere and thereby reduce the solar cycle variations in geopotential height, ozone, and temperature at tropical and subtropical latitudes [*Hood*, 2004]. *Field and Rishbeth* [1997] found that in cases they studied, geomagnetic activity produces greater

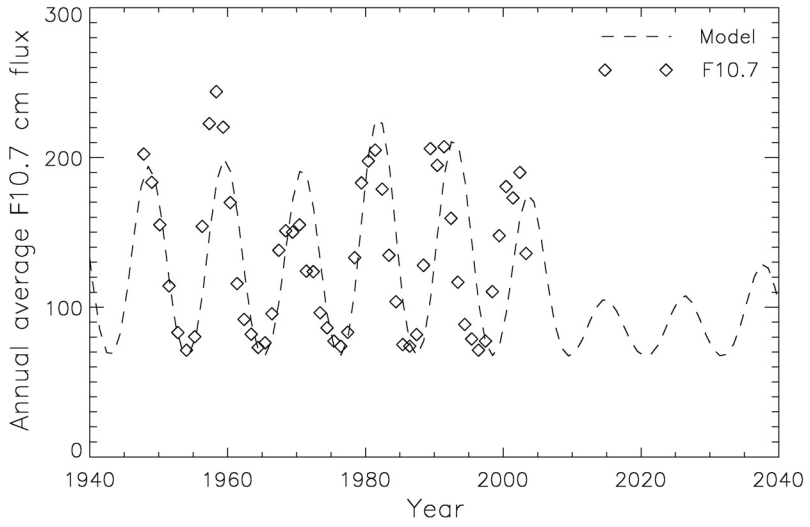

Figure 5. Comparison between the solar cycle averaged solar radio 10.7 cm flux converted from the low-frequency modulation model (dashed line) and the observed $F_{10.7}$ variation (diamonds) from 1947 to 2004.

relative depression of F_2 layer electron density in a solar cycle with lower $F_{10.7}$ than in ones of higher $F_{10.7}$.

4. Discussion and Summary

[20] We have used an extended model of low-frequency oscillations to represent the variation of sunspot number since 1750. The model involves the modulation of the 11.1-year Schwabe cycle by longer cycles with periods in the range 22–420 years. Typically, the standard deviation between the model and the peak sunspot number in each solar cycle is ±34. The prediction for cycle 24 is for a significantly quieter cycle than 23 with peak sunspot numbers of 42 ± 34. Long-term trends in the mismatch between model and observations indicate that the model is likely to underestimate the peak numbers for the next few cycles but within the error quoted. This result is in close agreement with the value of 50 predicted by *Badalyan et al.* [2001] on the basis of estimates from cyclic variations of the coronal green line intensities. These predictions suggest that a period of quiet solar activity is expected, lasting until ~2030, with a lower risk of disruption to satellite orbits, satellite lifetimes, and power distribution grids. Additionally, there should be a lower risk of spacecraft failures and less risk of high radiation dose to astronauts during this period [*Gorney*, 1990; *Shea and Smart*, 1998].

[21] The model also predicts a recovery during the middle of the present century to more typical solar activity cycles (peak sunspot numbers of ~120), in good agreement with the suggestions of *Kane* [2002], who considered the impact of a ~110-year oscillation (i.e., our 105-year cycle) in sunspot number data. In our study the superposition of the minimum phase of the 105- and 420-year cycles just after 2100 leads to another period of significantly quieter solar conditions. This lends some support to the prediction of low solar activity in 2100 made by *Clilverd et al.* [2003]. Figure 4 indicates that the minima will be about the same size as the Dalton Minima in 1805, thus representing the quietest solar activity conditions for 300 years.

[22] From long-term data such as the C^{14} series it is clear that low-frequency cyclic oscillations caused by solar activity are present [*Stuiver and Quay*, 1980; *Neftel et al.*, 1981; *Solanki et al.*, 2000; *Beer*, 2000]. The ΔC^{14} series shows that the Gleissberg period has been persistent over at least the last 12 kyr [*Peristykh and Damon*, 2003], and the Suess period was present for 25 kyr in the Greenland ice core [*Wagner et al.*, 2001]. Thus our periodic model uses cycles that are known to be persistent. Sometimes the long-period cycles driven by the solar dynamo can change phase [*Schove*, 1983], particularly during deep minima such as the Maunder Minimum, and may be representative of a chaotic Sun that shows periods of cyclic behavior that is ultimately unpredictable in the long term [*De Jager*, 2005; *Tobias et al.*, 2004]. However, it is clear that since the Maunder Minimum of 1700, the cycles used in the low-frequency modulation model described here have been present in the sunspot data, and as such, the model can provide a reasonable basis for predicting a few decades ahead as we have done in this paper.

[23] **Acknowledgment.** The authors would like to thank Hua Lu (BAS) and Neil Thomson (Otago University) for their useful discussions concerning this paper.

References

Ahluwalia, H. S. (1998), The predicted size of cycle 23 based on the inferred three-cycle quasi-periodicity of the planetary index *Ap*, *J. Geophys. Res.*, *103*, 12,103–12,109.

Badalyan, O. G., V. N. Obridko, and J. Sykora (2001), Brightness of the coronal green line and prediction for activity cycles 23 and 24, *Sol. Phys.*, *199*, 421–435.

Beer, J. (2000), Long-term indirect indices of solar variability, *Space Sci. Rev.*, *94*, 53–66.

Boteler, D. H. (2003), Geomagnetic hazards to conducting networks, *Nat. Hazards*, *28*, 537–561.

Clilverd, M. A., T. G. C. Clark, E. Clarke, and H. Rishbeth (1998), Increased magnetic storm activity from 1868 to 1995, *J. Atmos. Sol. Terr. Phys.*, *60*, 1047–1056.

Clilverd, M. A., E. Clarke, H. Rishbeth, T. G. C. Clark, and T. Ulich (2003), Solar activity in 2100, *Astron. Geophys.*, *44*, 20–22.

Cliver, E. W., V. Boriakoff, and J. Feynman (1998), Solar variability and climate change: Geomagnetic *aa* index and global surface temperature, *Geophys. Res. Lett.*, *25*, 1035–1038.

Conway, A. J., K. P. Macpherson, G. Blacklaw, and J. C. Brown (1998), A neural network prediction for cycle 23, *J. Geophys. Res.*, *103*, 29,733–29,742.

Damon, P. E., and J. L. Jirikowic (1992), The Sun as a low frequency harmonic oscillator, *Radiocarbon*, *34*, 199–205.

De Jager, C. (2005), Solar forcing of climate. 1: Solar variability, *Space Sci. Rev.*, *120*, 197–241.

De Meyer, F. (2003), A transfer function model for the sunspot cycle, *Sol. Phys.*, *217*, 349–366.

Dikpati, M., G. de Toma, and P. A. Gilman (2006), Predicting the strength of solar cycle 24 using a flux-transport dynamo-based tool, *Geophys. Res. Lett.*, *33*, L05102, doi:10.1029/2005GL025221.

Echer, E., N. R. Rigozo, D. J. R. Nordemann, and L. E. A. Vieira (2004), Prediction of solar activity on the basis of spectral characteristics of sunspot number, *Ann. Geophys.*, *22*, 2239–2243.

Field, P. R., and H. Rishbeth (1997), The response of the ionospheric F2-layer to geomagnetic activity: An analysis of worldwide data, *J. Atmos. Sol. Terr. Phys.*, *59*, 163–180.

Gholipour, A., C. Lucas, B. N. Araabi, and M. Shafiee (2005), Solar activity forecast: Spectral analysis and neurofuzzy prediction, *J. Atmos. Sol. Terr. Phys.*, *67*, 595–603.

Gleissberg, W. J. (1966), Ascent and descent in the eighty-year cycles of solar activity, *J. Br. Astron. Soc.*, *76*, 265–270.

Gorney, D. J. (1990), Solar cycle effects on the near-Earth space environment, *Rev. Geophys.*, *28*, 315–336.

Hood, L. L. (2004), Effects of solar UV variability on the stratosphere, in *Solar Variability and its Effects on Climate*, *Geophys. Monogr. Ser.*, vol. *141*, edited by J. M. Pap and P. Fox, pp. 283–303, AGU, Washington, D. C.

Kane, R. P. (2001), Did predictions of the maximum sunspot number for solar cycle 23 come true?, *Sol. Phys.*, *202*, 395–406.

Kane, R. P. (2002), Prediction of solar activity: Role of long-term variations, *J. Geophys. Res.*, *107*(A7), 1113, doi:10.1029/2001JA000247.

Kovaltsov, G. A., I. G. Usoskin, and K. Mursula (2004), An upper limit on sunspot activity during the Maunder Minimum, *Sol. Phys.*, *224*, 95–101.

Lockwood, M., R. Stamper, and M. N. Wild (1999), A doubling of the Sun's coronal magnetic field during the past 100 years, *Nature*, *399*, 437–439.

Neftel, A., H. Oeschger, and H. E. Suess (1981), Secular nonrandom variations of cosmogenic C-14 in the terrestrial atmosphere, *Earth Planet. Sci. Lett.*, *56*, 127–147.

Peristykh, A. N., and P. E. Damon (2003), Persistence of the Gleissberg 88-year solar cycle over the last 12,000 years: Evidence from cosmogenic isotopes, *J. Geophys. Res.*, *108*(A1), 1003, doi:10.1029/2002JA009390.

Schatten, K. H. (2003), Solar activity and the solar cycle, *Adv. Space Res.*, *32*, 451–460.

Schatten, K. H., D. J. Myers, and S. Sofia (1996), Solar activity forecast for solar cycle 23, *Geophys. Res. Lett.*, *23*, 605–608.

Schove, D. J. (1983), Sunspot, auroral, radiocarbon and climatic fluctuations since 7000 BC, *Ann. Geophys.*, *1*, 391–396.

Shea, M. A., and D. F. Smart (1998), Space weather: The effects on operations in space, *Adv. Space Res.*, *22*, 29–38.

Solanki, S. K., M. Schussler, and M. Fligge (2000), Evolution of the Sun's large-scale magnetic field since the Maunder Minimum, *Nature*, *408*, 445–447.

Sonett, C. P. (1982), Sunspot time series: Spectrum from square law modulation of the Hale cycle, *Geophys. Res. Lett.*, *9*, 1313–1316.

Stuiver, M., and T. F. Braziunas (1989), Atmospheric ^{14}C and century-scale oscillations, *Nature*, *338*, 405–408.

Stuiver, M., and P. D. Quay (1980), Changes in atmospheric carbon-14 attributed to a variable Sun, *Science*, *207*, 11–19.

Stuiver, M., P. J. Reimer, and T. F. Braziunas (1998), High-precision radiocarbon age calibration for terrestrial and marine samples, *Radiocarbon*, *40*, 1041–1083.

Svalgaard, L., E. W. Cliver, and Y. Kamide (2005), Sunspot cycle 24: Smallest cycle in 100 years?, *Geophys. Res. Lett.*, *32*, L01104, doi:10.1029/2004GL021664.

Tobias, S., N. Weiss, and J. Beer (2004), Long-term prediction of solar activity—A discussion, and a reply by Clilverd, M. A. et al., *Astron. Geophys.*, *45*, 2.6–2.7.

Usoskin, I. G., S. K. Solanki, and M. Schussler (2003), Millennium-scale sunspot number reconstruction: Evidence for an unusually active Sun since the 1940s, *Phys. Rev. Lett.*, *91*, 211101.

Vasillev, S. S., and V. A. Dergachev (2002), The ~2400-year cycle in atmospheric radiocarbon concentration: Bispectrum of ^{14}C data over the last 8000 years, *Ann. Geophys.*, *20*, 115–120.

Wagner, G., J. Beer, J. Masarik, R. Muscheler, P. W. Kubik, W. Mende, C. Laj, G. M. Raisbeck, and F. Yiou (2001), Presence of the solar de Vries cycle (~205 years) during the last ice age, *Geophys. Res. Lett.*, *28*, 303–306.

Walterscheid, R. L. (1989), Solar-cycle effects on the upper atmosphere—Implications for satellite drag, *J. Spacecr. Rockets*, *26*, 439–444.

E. Clarke, British Geological Survey, Natural Environment Research Council, West Mains Road, Edinburgh EH9 3LA, UK. (ecla@bgs.ac.uk)

M. A. Clilverd and M. J. Jarvis, British Antarctic Survey, Natural Environment Research Council, High Cross, Madingley Road, Cambridge CB3 0ET, UK. (macl@bas.ac.uk; mjja@bas.ac.uk)

H. Rishbeth, School of Physics and Astronomy, University of Southampton, Southampton SO17 1BJ, UK. (hr@phys.soton.ac.uk)

T. Ulich, Sodankylä Geophysical Observatory, University of Oulu, 99700 FIN-Sodankylä, Finland. (thu@sgo.fi)